

Human-in-the-Loop Optimization of Shared Autonomy in Assistive Robotics

Deepak Gopinath^{1,3}, Siddarth Jain^{2,3} and Brenna D. Argall^{2,3}

Abstract—In this paper, we propose a mathematical framework which formalizes user-driven customization of shared autonomy in assistive robotics as a nonlinear optimization problem. Our insight is to allow the *end-user*, rather than relying on standard optimization techniques, to perform the optimization procedure, thereby allowing us to leave the exact nature of the cost function indeterminate. We ground our formalism with an interactive optimization procedure that customizes control sharing using an assistive robotic arm. We also present a pilot study that explores interactive optimization with end-users. This study was performed with 17 subjects (4 with spinal cord injury, 13 without injury). Results show all subjects were able to converge to an assistance paradigm, suggesting the existence of optimal solutions. Notably, the amount of assistance was not always optimized for task performance. Instead, some subjects favored retaining more control during the execution over better task performance. The study supports the case for user-driven customization and provides guidance for its continued development and study.

I. INTRODUCTION

For people with severe motor impairments as a result of spinal cord or brain injuries, assistive and rehabilitation machines such as assistive robotic arms, upper or lower limb prostheses and powered wheelchairs are crucial for reducing their dependence on caretakers and increasing the ability to perform activities of daily life. However, for many, the control of such devices remains a challenge—for example, due to their physical impairments or limitations of the control interfaces. Such interfaces often issue control signals that are low-dimensional, discrete and operate in different modes, each of which correspond to different parts of the control space that must be switched between. The introduction of partial autonomy to these devices—in which the control is shared between the human and robotics autonomy—aims to help reduce the cognitive and physical burden on the user.

The reduced bandwidth of the control signals generated by motor-impaired users makes them more reliant on the interaction with the autonomy, and also less adaptable and more vulnerable to any arbitrariness present in the system—for example, the choice of control interfaces and mappings, or the exact specification of how control is shared between the user and the autonomy. A thorough analysis of user performance and the differences in performance between uninjured

and motor-impaired subjects calls for a rich mathematical framework that can capture the various facets of the shared control system, like the complex dynamics of the human-robot interaction. *Furthermore*, the exact formulation used to describe the human-robot interaction will determine (or limit) the relevant and valid questions that can be asked and how the analysis of performance metrics will be performed. To accomplish this, we introduce a mathematical formalism in which the customization procedure is formulated as a nonlinear optimization problem over system parameters.

Since users differ in their physical abilities and desired amount of assistance, *customization* of the amount of assistance is critical for the adoption of assistive shared-control systems. Predefined assistance levels can provide good starting points but may not remain optimal for the user in the long term. For example, the subject’s abilities will likely be changing—either degrading (e.g. due to degenerative disease) or improving (e.g. due to successful rehabilitation). As a result of which the need for assistance may be increased or decreased. One way to accomplish customization is to tune the system parameters which will bring about a change in the human-robot interaction and the final behavior. The aim is to optimize the human-robot interaction during task performance. A simple choice of optimality criterion is to consider task-related performance metrics such as minimizing the time taken and energy expended.

Our insight is that if we entrust the task of customization to the users, they likely will tune the system in such a way that the optimal interaction—according to their personal optimality criterion—will emerge. Moreover, the user-driven customization of assistance may be task-dependent in addition to being user-dependent.

To ground our formalism, we present a first implementation, in which the reasoning between the user control and the robot policy is a function of confidence in the inference of human intent, with tunable parameters. Our interactive user-driven customization system maps verbal cues from the human to adjustments in these parameter values. Results from an exploratory pilot study also are presented.

In Section II we present an overview of the relevant research in the field of shared control systems in assistive technology. Section III overviews of the general algorithm and system design used in this study. The system implementation is described in Section IV and Section V provides an overview of the user study methods, tasks and metrics used. In Section VI we present the results from our pilot study and discussion followed by conclusions in Section VII.

¹Department of Mechanical Engineering, Northwestern University, Evanston, IL, 60208, USA

²Department of Electrical Engineering & Computer Science, Northwestern University, Evanston, IL, 60208, USA

³Rehabilitation Institute of Chicago, Chicago IL, 60211 USA
deepakedakkattilgopinath2015@u.northwestern.edu
sidd@u.northwestern.edu
brenna.argall@northwestern.edu

II. RELATED WORK

The introduction of robotics autonomy to assistive devices can offload some control burden from users to enable easier operation. While full autonomy is an option, more common are systems that share control with the human user—for reasons of both robustness [1] and user preference [2].

The most common methods to share control between the user and autonomous system include (a) the user selects the higher-level goal and the autonomy generates the lower-level control, (b) control partitioning schemes and (c) blending the user controls and the autonomy commands. In the domain of robotic wheelchair research, the higher-level goals typically are navigation goals [3], while control partitioning for example places the control of speed with the user and heading with the autonomy [4]. Control blending paradigms often are employed for behaviors like obstacle avoidance [5]. Control sharing in case of robotic arms most commonly involves user-specification of a target (such as an object) [6] or pose correction [7], with the robot autonomously generating the motion commands. Approaches that partition the control space may, for example, place the control of end-effector position in z with the human and in x, y with the autonomy [8]. Control blending is less straightforward—because the user rarely is able to issue a control signal with high enough dimensionality to cover all control dimensions of the robot (e.g. 6D)—but recently is gaining interest.

Moreover, there are approaches which study specifically the customization of how this control blending happens [9]. The amount of control blending often is determined using an arbitration function that is based, for example, on the autonomy’s confidence in its prediction of the user’s goal [10]. Our work similarly employs an arbitration function to dictate the amount of control sharing.

Optimization techniques have been adopted to generate different strategies for control sharing; for example, formulating the problem as a POMDP and inferring a distribution over goals from user commands via Maximum Entropy Inverse Optimal Control [11], using pseudo-navigation functions for collaborative control in robotic wheelchairs [12] or concatenating energy-optimal motion primitives to create optimal trajectories [13]. Although these approaches result in improved task performance (task completion time, control effort), the assistance schemes are mixed in terms of user acceptance. In particular, there are instances of assistance resulting in higher user dissatisfaction [11], and users preferring to be in control and more cautious [13]. In other studies users find the assistance at times to be uncooperative and are willing to tolerate a loss of control only when there is a significant improvement in performance [14].

In an attempt to construct more realistic cost functions, other researchers incorporate a measure of “discomfort” into the optimization cost function. Inspired by research in design (transportation, elevator etc.) a discomfort cost function is formulated [15], however, the specific form of the cost function is domain dependent and is not generalizable to other assistive devices such as robotic arms.

Despite an improvement in task performance, none of the above cost function formulations were able to guarantee high user satisfaction (with the exception of domain-specific [15]). The need for higher user satisfaction is crucial for the acceptance of robot autonomy by the end-users in the assistive domain. This gap motivates our approach to engage the end-user in the optimization procedure.

III. PROPOSED FRAMEWORK

Principles from optimal control theory have been successfully used to account for different aspects of human motor control such as arm trajectory formation, posture control and locomotion [16], [17], [18]. The underlying motivation in using optimal control theory is that biological systems have evolved to produce motor commands which will optimize motor behavior with respect to the task at hand [18]. When a human operates an assistive robot to replace his/her lost motor function, the extension of this reasoning is that the optimizing principles are operating over control commands to the robot effector rather than motor commands to the human muscles. We frame our formalism within the language of optimal control theory not only because of this biological parallel, but also because it will allow for the analysis of the effects of the various design decisions in and components of a shared control system in a thorough and rigorous manner.

A. Formalism

Let $\mathbf{x}(t)$ denote the state of the system at time t . Let $\boldsymbol{\theta}(t)$ be the set of tunable parameters that will affect the amount of control shared between the human and the robot. The other control inputs to the system are $\mathbf{u}_h(t)$ and $\mathbf{u}_r(t)$, the control commands generated respectively by the user and autonomous robot policy at time t .

The control signal from the robot autonomy is generated by a function $f(\cdot) \in \mathcal{F}$,

$$\mathbf{u}_r(t) \leftarrow f(\mathbf{x}(t)) \quad (1)$$

where \mathcal{F} is the set of all control behaviors corresponding to different tasks.

We assume that the control command $\mathbf{u}_h(t)$ is generated by a function of $g(\cdot) \in \mathcal{G}$,

$$\mathbf{u}_h(t) \leftarrow g(\mathbf{x}(t)) \quad (2)$$

where \mathcal{G} is the set of user behaviors corresponding to different tasks. $g(\cdot)$ is simply a symbolic representation of the mapping function that generates $\mathbf{u}_h(t)$ and is completely unknown to the autonomous system. The sole dependence of $\mathbf{u}_h(t)$ on $\mathbf{x}(t)$ is an approximation because there may be a large number of unobserved variables (e.g fatigue or personal satisfaction) affecting the user’s decision.

The shared control system makes use of function $\beta(\cdot)$, parameterized by $\boldsymbol{\theta}$

$$\mathbf{u}(t) \leftarrow \beta_{\boldsymbol{\theta}}(\mathbf{u}_h(t), \mathbf{u}_r(t)) \quad (3)$$

which arbitrates between the control commands from the user and the robot policy to produce control command $\mathbf{u}(t)$ executed by the robot.

A key insight in our formulation is that, for a time-varying function $\beta(\cdot)$, the parameters themselves can be functions of time and therefore may be interpreted as control signals. Then the dynamics of the system can be written as

$$\dot{\mathbf{x}}(t) \leftarrow \mathbf{a}(\mathbf{x}(t), \boldsymbol{\theta}(t), \mathbf{u}_h(t), \mathbf{u}_r(t), t) \quad (4)$$

where $\mathbf{a}(\cdot)$ is in general a non-linear, time-varying function. Note that in this formulation the parameters $\boldsymbol{\theta}(t)$ are treated in the *same way* as the other control signals. The problem of finding the set of parameters $\boldsymbol{\theta}(t)$ that will generate the optimal human-robot interaction and task performance (as determined by a cost function) thus may be formulated as an optimal control problem.

Optimal control models assume the existence of some kind of cost function being optimized during task performance.¹ In general, the cost function J can be written as,

$$J \leftarrow \mathbf{h}(\mathbf{x}(t_f), t_f) + \int_{t_0}^{t_f} \mathbf{k}(\mathbf{x}(t), \mathbf{u}(t), t) dt \quad (5)$$

where the first term corresponds to a terminal cost (e.g proximity of the end pose to the target pose) and the second term corresponds to a measure of internal cost (e.g the energy expended during task execution, task completion time, etc). The true cost function, however likely is more complex, and could include additional factors such as user satisfaction. The state boundary conditions are given by $\mathbf{x}(t_0) = x_0$ and $\mathbf{x}(t_f) = x_f$ where, t_0 and t_f are the times at which the robot is in the initial state x_0 and final state x_f . The parameter constraints are $\boldsymbol{\theta}_{min} \leq \boldsymbol{\theta}(t) \leq \boldsymbol{\theta}_{max}$.

The elements of the framework $f(\cdot)$, $g(\cdot)$, $\beta(\cdot)$ and $\mathbf{a}(\cdot)$ are system-specific, and different choices of these functions will have drastically different impact on task performance and user satisfaction. Moreover, the impact is anticipated to be all the greater on motor-impaired subjects.

B. Optimization

Typically optimization is performed over all control signals that are inputs to the system. In our system, however, the control commands from the human and the robot ($\mathbf{u}_h(t)$, $\mathbf{u}_r(t)$) are treated as given quantities, and the goal rather is to optimize the interaction parameters $\boldsymbol{\theta}(t)$. Therefore, optimization is performed only with respect to a subspace ($\boldsymbol{\theta}(t)$) of the entire control space.

In this work, we furthermore make no attempt to determine the exact nature of the cost function J . There might be a myriad of unmeasurable factors influencing the cost function, and determining the exact mathematical form for the cost function likely is an intractable problem. Making any kind of approximation to simplify the cost function in turn will affect the robustness and efficacy of the assistive system. Since we do not want to reduce the assistive capabilities of our system, and we have a human in the loop, our

¹For example, arm trajectories generated by uninjured humans during reaching tasks have been reproduced using a cost function composed of total torque generated at the joints [16] or total jerk of the end effector (hand) [17].

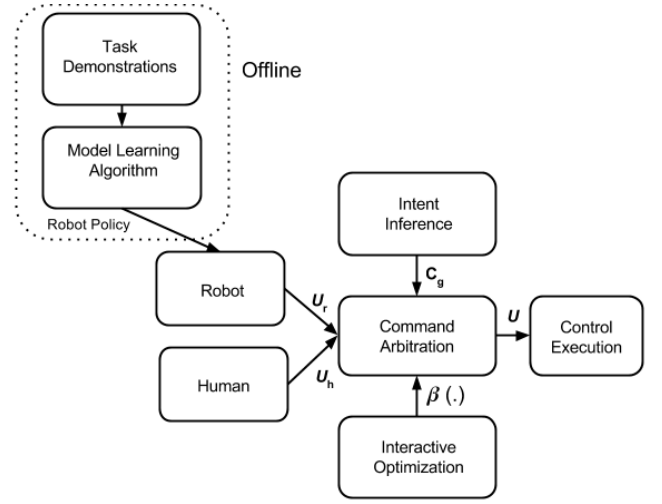


Fig. 1. System design. Core components include command arbitration and the interactive optimization of how this arbitration happens.

insight is that the optimization task can be performed by the user him/herself, instead of adopting standard non-linear optimization algorithms. Thus there is no need to concretely define J and the user tunes the parameters $\boldsymbol{\theta}(t)$ until optimal behavior is achieved.

In this user-driven customization system, the overall effect of parameter tuning is that of changing the assistance offered by the robot. The exact specifics of the optimization procedure is described in detail in Section IV-B.

IV. SYSTEM IMPLEMENTATION

Our system implementation is overviewed in Figure 1. The key components of this system include the command arbitration paradigm (Sec. IV-A), the user-driven optimization procedure (Sec. IV-B) and the estimation of human intent (Sec. IV-C). Also provided are details of how the human control signals are acquired (Sec. IV-D) and the robot autonomy commands are generated (Sec. IV-E).

A. Command Arbitration

In our implementation, the function $\beta(\cdot)$ that reasons between the robot and human control signals is a linear blending function,

$$\beta_{\boldsymbol{\theta}}(\mathbf{u}_h(t), \mathbf{u}_r(t)) \triangleq (1 - \alpha_{\boldsymbol{\theta}}) \cdot \mathbf{u}_h(t) + \alpha_{\boldsymbol{\theta}} \cdot \mathbf{u}_r(t) \quad (6)$$

where $\alpha_{\boldsymbol{\theta}} \in [0, 1]$ is itself a function parameterized by $\boldsymbol{\theta}$.² Note that $\alpha_{\boldsymbol{\theta}} = 0$ corresponds to full teleoperation, and $\alpha_{\boldsymbol{\theta}} = 1$ to full autonomy.

The majority of *arbitration functions* $\alpha_{\boldsymbol{\theta}}$ can be reduced to the functional form pictured in Figure 2 [10]. This particular function is characterized by a set of three parameters $\{\theta_1, \theta_2, \theta_3\}$ and independent variable $c(t)$. The parameter set determines:

- θ_1 : The minimum value of $c(t)$ above which control blending is performed.

²The time index t is dropped from $\boldsymbol{\theta}(t)$ for brevity in notation.

Verbal Cue	Parameters Changed	Amount of change
“More”	$\theta_3 \uparrow, \theta_2 \downarrow, \theta_1 \downarrow$	$\delta\theta \leftarrow \delta\theta$
“Less”	$\theta_3 \downarrow, \theta_2 \uparrow, \theta_1 \downarrow$	$\delta\theta \leftarrow \delta\theta$
“Little More”	$\theta_3 \uparrow, \theta_2 \downarrow, \theta_1 \uparrow$	$\delta\theta \leftarrow \frac{1}{2}\delta\theta$
“Little Less”	$\theta_3 \downarrow, \theta_2 \uparrow, \theta_1$ (no change)	$\delta\theta \leftarrow \frac{1}{2}\delta\theta$

TABLE I

MAPPINGS FROM VERBAL CUES TO PARAMETERS CHANGED
(\uparrow indicates a positive $\delta\theta$ and \downarrow denotes a negative $\delta\theta$)

- θ_2 : The value of $c(t)$ above which the blending parameter is maximum and constant.
- θ_3 : The maximum value of α for any value of $c(t)$.

Note that $\theta_3 = 0$ corresponds to constant teleoperation (irrespective of the value of $c(t)$). The relationship between $c(t)$ and α_θ is linear between θ_1 and θ_2 , and the slope of this linear relation determines how aggressively the robot assumes control. The parameter bounds are such that $\forall i, \theta_i(t) \in [0, 1]$ and $\theta_1 \leq \theta_2$. The independent variable $c(t)$ in our implementation is discussed in Sec IV-C.

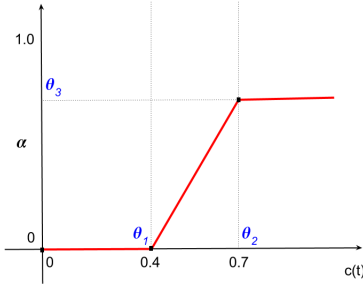


Fig. 2. A prototypical arbitration function, parameterized by $\theta = \{\theta_1, \theta_2, \theta_3\}$.

In our pilot study, the parameters were tuned only between tasks and were unchanged during task execution, and so $\theta_i(t) = \theta_i(t_0), \forall t \in [t_0, t_f]$. The arbitrated signal $\mathbf{u}(t)$ was the final velocity of the end-effector in Cartesian space, converted to joint-space velocities via inverse kinematics.

B. User-Driven Optimization of the Arbitration Parameters

In this first exploration of our interactive optimization procedure, verbal commands from the human subject are translated to changes in θ by the system operator. The interactive optimization procedure is currently being formalized and automated, as informed by this pilot data.

A change in assistance level can be achieved by modulating one or more of the $\theta_i \in \theta$, according to $\theta_i = \theta_i \pm \delta\theta_i$. In our implementation, at initialization $\delta\theta_i = 0.1$. The value of $\delta\theta_i$ is adaptive, and is halved if a request to increase assistance is immediately followed by a request to decrease and vice versa (in order to avoid oscillatory behavior).

Table I provides a few example mappings between common verbal cues, the parameters changed and the values of $\delta\theta$. We chose to modulate more than one parameter at a time as it helped to make the change in assistance level more perceivable to the user.

C. Estimation of Intent

In our implementation, the independent variable $c(t)$ of the arbitration function is the autonomous system’s confidence in its inference of the intent (goal) of the human. The confidence $c(t)$ is computed at each execution step that the

Control Mappings		
Mode	3D	2D
1	v_x, v_y, v_z	v_x, v_y
2	$\omega_x, \omega_y, \omega_z$	v_x, v_z
3	—	ω_x, ω_y
4	—	ω_z

TABLE II

OPERATIONAL PARADIGMS FOR THE TELEOPERATION INTERFACE

human provides a control signal, i.e. $\mathbf{u}_h(t) \neq \emptyset$. In our implementation, $c(t)$ is computed as

$$c(t) \triangleq \mathbf{w}_1(\mathbf{u}_h(t) \cdot \mathbf{u}_r(t)) + \mathbf{w}_2(e^{-d}) \quad (7)$$

where d is the Euclidean distance between the end effector and an inferred target location at time t , and $c(t) \in [0, 1]$. The first term in (7) provides a measure of agreement between the user-generated commands and robot-generated commands. The second term encodes the nearness to the target. Parameters \mathbf{w}_1 and \mathbf{w}_2 are task-specific weights.³

At each execution step this confidence measure is computed for all candidate goals in the scene, $\lambda \in \Lambda$, resulting in a distribution of confidences $c_\lambda(t) \in \mathcal{C}$ over the candidate goals.⁴ To compute these confidences, each control behavior f_λ generates a command (where f_λ aims to reach candidate goal λ) which is used in the calculation of $c_\lambda(t)$ according to (7). The command associated with the target that has the highest computed confidence is selected.

D. Control Interface and Mapping

The human control command $\mathbf{u}_h(t)$ is captured via a teleoperation interface, that consists of a 3-axis joystick operated under two different mapping paradigms (Table II). The joystick signals are mapped to the translational and rotational velocities of the end-effector in Cartesian space. The first paradigm uses only two of the three axes (no twist)—because many end-users lack the hand function to perform twisting—and accordingly defines four 2D modes to cover the six control dimensions of the robot arm. We refer to this as the *2D mapping paradigm*. The second uses all three of the joystick axes under two 3D operational modes and is referred to as the *3D mapping paradigm*.

E. Derivation of the Autonomy Policy

The robot control command $\mathbf{u}_r(t)$ is generated from an autonomous control policy. While any number of techniques may be employed to derive the behavior functions in \mathcal{F} , there are some limitations on the form that f should take. Attempting to return the robot to the pre-planned path (as many planners do) does not make sense in shared-control systems where the sources of deviations are human commands—this likely would be unwelcome to the user. Instead replanning would need to happen fast enough not to stall the task execution. We therefore advocate the use of

³Prior to computing $c(t)$ the control commands $\mathbf{u}_h(t)$ and $\mathbf{u}_r(t)$ are smoothed using a moving average filter (0.6s), so that small command changes do not affect the confidence measure drastically.

⁴In this study the candidate goals are objects placed at predefined positions in front of the robot. Our system is also able to autonomously perceive object positions and use these as candidate goals.



Fig. 3. Study tasks performed by an spinal cord injury (SCI) participant. *Left to right*: Simple Reaching (R), Reaching for Grasping (RfG), Reaching for Scooping (RfS).

real-time control policies which are defined in all parts of the state space.

Our current implementation favors dynamical systems formulations. The autonomous robot policies are derived from human demonstrations using a Learning from Demonstration approach known as *Stable Estimator of Dynamical Systems* (SEDS) [19]. In SEDS, the target poses are modeled as attractors of a dynamical system. For each task, a set of N demonstrations are collected by kinesthetically moving the robot. Demonstrations consist of pairs of joint angles $\mathbf{x}(t) \in \mathbb{R}^6$ and joint velocities $\dot{\mathbf{x}}(t) \in \mathbb{R}^6$. The SEDS algorithm learns the parameters of a time-independent dynamical system which models the joint velocities as a function of joint angles, and so

$$\dot{\mathbf{x}}(t) \leftarrow f(\mathbf{x}(t)) \quad (8)$$

where $\mathbf{u}_r(t) \triangleq K(\dot{\mathbf{x}}(t))$ and $K(\cdot)$ is the forward kinematics of the robot arm (since human teleoperation and control blending both happen in the end-effector Cartesian space). The dynamical system ensures that the policy exists everywhere in the workspace, and that the robot trajectories follow the general contour of the task demonstrations.

V. PILOT STUDY METHODS

The experiments were performed using the MICO robotic arm (Kinova Robotics, Canada) which is specifically designed for assistive purposes. The system was implemented using the Robot Operating System (ROS) and model learning was performed using MATLAB. The maximum end effector translational velocity along any axis was capped at 20 cm/s.

A. Task Descriptions

Three tasks were developed for our pilot study (Fig. 3).

Simple Reaching (R): The user teleoperates the robotic arm to reach a single object (coffee carafe) placed in front of the robotic arm. The purpose of this task is to get the user accustomed to the control interface and to the different assistance levels provided by the system. At the end of the task, the assistance level that the user preferred was noted.

Reaching for Grasping (RfG): The user teleoperates the robotic arm to reach one of two objects on the table with a pose suitable for grasping, as the robot arm provides assistance. There is a near object (mug) and a far object (box),

each of which requires a different orientation of the gripper for grasping (side and top, respectively) and accordingly also different approach trajectories during reaching.

Reaching for Scooping (RfS): The user teleoperates the robotic arm to reach for one of two objects on the table with a pose suitable for a scooping motion, as the robot arm provides assistance. There is a near object and a far object (both bowls), each of which requires a different approach trajectory. For this task, the end effector of the robotic arm is fitted with a spoon which must be inserted into the bowl.

B. Study Protocol and Metrics

Subjects: For this exploratory study 17 subjects were recruited—13 uninjured control subjects (mean age: 26 ± 4 , 8 males and 5 females) and 4 SCI subjects (mean age: 35 ± 14 , all males, C3-C5 injury levels). Seven of the uninjured subjects (5 males, 2 females) and 3 of the SCI subjects used the 3D interface paradigm, and the remaining subjects used the 2D paradigm. All participants gave their informed, signed consent to participate in this experiment, which was approved by Northwestern University’s Institutional Review Board.

Protocol: Each user performed all three tasks. The purpose of the practice task (R) was to get the user accustomed to the control interface and assistance system. Data was then collected on the remaining two tasks (RfG, RfS). The order of presentation for the RfG and RfS tasks was randomized and balanced across subjects, to avoid ordering effects.

Before the RfG and RfS trials, the user was first asked to operate the system in full teleoperation mode (*tel*) and also under three predefined assistance levels (*min*, *mid* and *max*). After this phase, the subject was given the option to customize the assistance level. Changes in assistance levels were communicated verbally to the system operator resulting in the parameter changes outlined in Table I. The user then tested the customized assistance level by executing the task. This customization procedure was repeated until the user was satisfied and lasted on average 10 and a maximum of 15 minutes, resulting in assistance level *custom*. Data collection began only after this customization process was completed. Three trials were collected for *min*, *max* and *custom* assis-

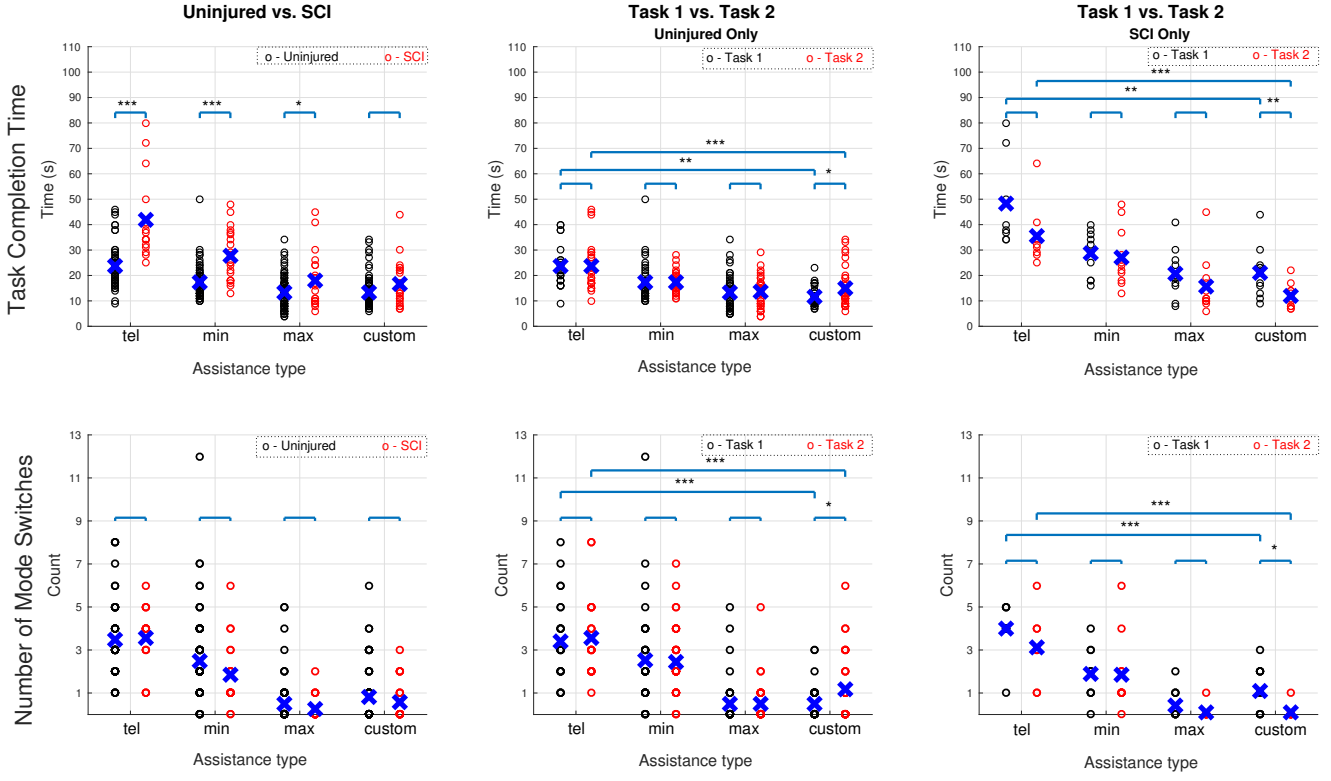


Fig. 4. Task completion time (top row) and number of mode switches (bottom row) for uninjured vs. SCI subjects (first column), Task 1 vs. Task 2 for uninjured subjects only (second column), Task 1 vs. Task 2 for SCI subjects only (third column).

tance levels.⁵ A typical session lasted approximately 1-1.5 hours. For the first (non-practice) task, the baseline from which customization began was the *mid* level assistance, with level *custom* being the result after customization. For the second task, customization began at this level *custom* from the first task as the baseline, with the option to further customize resulting in level *custom* for the second task.

Metrics: A number of objective metrics evaluated this study. *Task Completion time* is the amount of time spent accomplishing a task. *Mode Switches* refer to the number of times the subject switched between the various modes of the control interface (Table II). Mode switch additionally is an indirect measure of the effort put forth by the user. At the end of the study, subjective data was gathered via a brief questionnaire. To explore subject opinions, users were given statements about the assistance system, and asked to rate each one of them on a 7-point Likert scale (1 is low, 7 is higher), according to their agreement. The questions primarily concerned the utility value of the assistance system (*UI*), the system's accuracy in goal perception (*CA1*) and its understanding of what the user is trying to accomplish (*CA2*) and the contribution from the user (*CO1*) and the system (*CO2*) in task accomplishment.

⁵For one SCI participant one less trial was recorded for *min* assistance level during the first task due to a clerical error.

VI. RESULTS

Here we report the results of our pilot study. An improvement in task performance with customization is demonstrated, and a number of other interesting observations are noted. Task performance metrics for different assistance levels (denoted by *min*, *max* and *custom* in the plots) and teleoperation (*tel*) are analyzed across different subject groups, tasks and control interfaces. Note that the *custom* assistance level always lies in between (or is equal to) *min* and *max*. Statistical significance is determined by Welch t-tests for Figures 4-5 and two sided Wilcoxon Rank-Sum Test for Figure 6, where (***) indicates $p < 0.001$, (**) $p < 0.01$ and (*) $p < 0.05$.

A. Observations across Uninjured and SCI subjects

Insight into Cost Function: Figure 4 (first column) represents the task completion time (top) and mode switches (bottom) for uninjured and SCI subject groups, averaged across all tasks and interface mapping paradigms. For the *custom* assistance type, task completion times are comparable to those of the *max* assistance type. However, the number of mode switches for *custom* is *greater* than those of *max* (though this effect is not statistically significant). Thus, it is not uniformly the case that mode switches are minimized from low to high assistance.

This provides insight that the true cost function that the user is optimizing is more complex than a simple time-optimal or minimum-effort cost function.

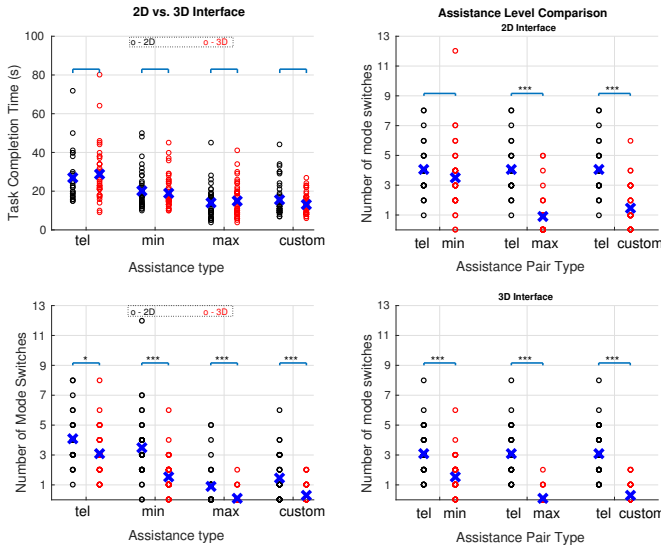


Fig. 5. Left Column: Task completion time (top) and number of mode switches (bottom) for the 2D vs. 3D interfaces. Right Column: Within-interface assistance level comparison for the 2D (top) and 3D (bottom) interfaces.

Task Performance: In Figure 4 (first column), the difference between task completion times for uninjured and SCI subjects drops steadily from *tel* to *custom* assistance levels. The t-tests revealed that while the difference between uninjured and SCI was statistically significant for both *tel* ($p = 5.1e-4$) and *min* ($p = 6.5e-5$), this difference disappeared with the *max* ($p = 0.027$) and *custom* ($p = 0.096$) assistance levels. That is, with increased assistance, the performance of SCI subjects was comparable to that of uninjured subjects and this was *maximized* under customization. The variance in the data also *decreases* with customized assistance, showing the performance to become more consistent.

Interestingly, for mode switches there was no statistical difference between uninjured and SCI subject data for any of the assistance levels. This suggests that the number of mode switches is primarily determined by the nature of the task and control interface, and not the state of injury. However, SCI subjects do take more time than uninjured subjects to perform the same number of mode switches.

B. Observations across Tasks

Figure 4 (second and third columns) shows how task completion times and number of mode switches change between the first and second task. For uninjured subjects, there was no change in performance over trials, and neither between different assistance levels for either metric. The same was true for SCI subjects with the *exception* of the *custom* level. Specifically SCI subjects saw an improvement in task completion times ($p = 7.8e-3$) and mode switches ($p = 8.9e-3$) between the first and second tasks for the *custom* assistance level. There is also significant improvement in task completion times ($p = 3.2e-3$ for Task 1 and $p = 8.2e-4$ for Task 2) and mode switches ($p = 1.6e-4$ for Task 1 and $p = 4.9e-5$ for Task 2) for levels *tel* and *custom*.

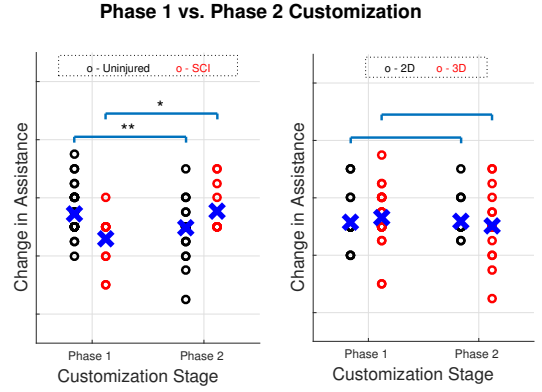


Fig. 6. Relative change in assistance parameters during customization for Uninjured vs. SCI subjects (left) and 2D vs. 3D subjects (right).

C. Observations across Control Interfaces

The first column of Figure 5 shows the task completion times and mode switches for subjects using the 2D and 3D interfaces. Different operational modes do not seem to have an effect on task completion times, as both groups are statistically equivalent—*despite* the fact that for mode switches the difference between the 2D and 3D interfaces is significant (except for *tel*). The second column of Figure 5 shows a *within-interface* performance comparison between *tel* and the different assistance levels. For all levels assistance significantly helped in reducing the number of mode switches during task execution.

The comparable task completion times may be explained by the fact that easier control compensates for time lost during mode switches. That is, due to the greater number of mode switches required for the 2D interface compared to the 3D interface, more time is taken performing mode switches. However, the number of dimensions simultaneously controlled is less for the 2D interface compared to the 3D interface, which makes the control easier.

D. Relative Change in Parameters during Customization

Figure 6 shows the change in amount of assistance during customization for uninjured and SCI subjects. While SCI subjects on average increased the amount of assistance ($p = 0.02$) during the second phase of customization, uninjured subjects chose to reduce the amount of assistance ($p = 0.006$). There were no noticeable changes in the customized assistance levels between the 2D and 3D interfaces. Injury seems to be the primary reason why subjects choose to change the customized assistance levels and the mapping paradigm seem to have little effect.

E. User Survey

Users rated the utility value of the assistance system fairly high (mean = 5.9 ± 0.8) indicating that in general having assistance was favored. The users also thought that the system was able to perceive goals quite accurately (mean = 5.1 ± 1.8) and the inability to estimate human intent was fairly low (mean = 3.1 ± 1.1). The users also felt that they played an important part in accomplishing the task (mean

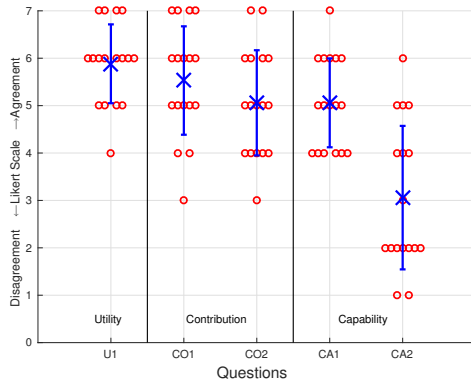


Fig. 7. User questionnaire responses. User questionnaire responses.

$= 5.5 \pm 1.0$), almost comparable to the contribution from assistance (mean $= 5.1 \pm 1.6$), maybe indicating that they were not prepared to relinquish control altogether (Fig. 7).

F. Discussion

From our pilot study we saw that compared to pre-defined assistance levels, customization improves task performance and helps to reduce performance differences between uninjured and SCI subjects. Post-experiment surveys also revealed that the users found the customized assistance paradigm to be useful. These results establish a need for customization of assistance levels. Therefore, our next step will be to explore multiple possibilities for building effective and intuitive customization mechanisms (for example, physical interfaces operated by the user) which will suit individual requirements and preferences and to evaluate on a larger end-user population. The results also show that the true cost function that is being optimized is more complex than a simple time-optimal or minimum-effort cost function indicating the need to investigate the exact specification of the true cost function that is being optimized by the human in a shared control system. A more comprehensive user survey will also be administered in which the formalized customization procedure will be evaluated thoroughly.

VII. CONCLUSIONS

In this work, we formalize human robot interaction in shared autonomy within the framework of optimal control theory. Furthermore we have also introduced a system for user-driven customization which is presented as a constrained non-linear optimization problem within this framework. Unlike standard optimization problems in which the form of the cost function is predetermined in this work no such assumptions were made. Instead, the end user was allowed to directly perform the optimization procedure. The aim is that this will lead to higher user satisfaction, which is crucial for the acceptance of novel technologies in the assistive domain. An interactive user-driven customization system was also developed to ground the formalism and the results from the pilot study were also presented. Results showed that all subjects were able to converge to a optimal assistance paradigm and an improvement in task performance with customization was also demonstrated.

ACKNOWLEDGMENTS

Many thanks to Jessica Presperin Pedersen, OTR/L, ATP/SMS, for recruiting the SCI subjects, and to Samuel Schlesinger for assistance during the subject studies. Research reported in this publication was supported by the NIBIB & NICHD under award number R01EB019335. The content is solely the responsibility of the authors and does not necessarily represent the official views of the NIH.

REFERENCES

- [1] I. Volosyak, O. Ivlev, and A. Gräser, "Rehabilitation robot FRIEND II - the general concept and current implementation," in *International Conference on Rehabilitation Robotics (ICORR)*, 2005.
- [2] D.-J. Kim, R. Hazlett-Knudsen, H. Culver-Godfrey, G. Rucks, T. Cunningham, D. Portee, J. Bricout, Z. Wang, and A. Behal, "How autonomy impacts performance and satisfaction: Results from a study with spinal cord injured subjects using an assistive robot," *IEEE Transactions on Systems, Man and Cybernetics, Part A: Systems and Humans*, vol. 42, no. 1, pp. 2–14, 2012.
- [3] R. Simpson, "Smart wheelchairs: A literature review," *Journal of Rehabilitation Research & Development*, vol. 42, no. 4, pp. 423–438, 2005.
- [4] R. Simpson, S. Levine, D. Bell, L. Jaros, Y. Koren, and J. Borenstein, "NavChair: An assistive wheelchair navigation system with automatic adaptation," in *Assistive Technology and Artificial Intelligence*, vol. 1458 of *Lecture Notes in Computer Science*, pp. 235–255, 1998.
- [5] T. Carlson and Y. Demiris, "Collaborative control for a robotic wheelchair: Evaluation of performance, attention and workload," *IEEE Transactions on Systems, Man, and Cybernetics: Part B*, vol. 42, no. 3, pp. 876 – 888, 2012.
- [6] A. Jain and C. C. Kemp, "El-e: an assistive mobile manipulator that autonomously fetches objects from flat surfaces," *Autonomous Robots*, vol. 28, no. 1, pp. 45–64, 2010.
- [7] Z. Bien, M.-J. Chung, P.-H. Chang, D.-S. Kwon, D.-J. Kim, J.-S. Han, J.-H. Kim, D.-H. Kim, H.-S. Park, S.-H. Kang, K. Lee, and S.-C. Lim, "Integration of a rehabilitation robotic system (KARES II) with human-friendly man-machine interaction units," *Autonomous Robots*, vol. 16, no. 2, pp. 165–191, 2004.
- [8] B. J. F. Driessen, T. K. T. Kate, F. Liefhebber, A. H. G. Versluis, and J. A. van. Woerden, "Collaborative control of the manus manipulator," *Universal Access in the Information Society*, vol. 4, no. 2, pp. 165–173, 2005.
- [9] Q. Li, W. Chen, and J. Wang, "Dynamic shared control for human-wheelchair cooperation," in *Proceedings of the International Conference on Robotics and Automation (ICRA)*, 2011.
- [10] A. Dragan and S. Srinivasa, "Formalizing assistive teleoperation," in *Proceedings of Robotics: Science and Systems*, 2012.
- [11] S. Javdani, S. Srinivasa, and A. Bagnell, "Shared autonomy via hindsight optimization," in *Proceedings of Robotics: Science and Systems*, 2015.
- [12] M. Fernández-Carmona, J. M. Peula, C. Urdiales, and F. Sandoval, "Towards a shared control navigation function: efficiency based command modulation," in *International Work-Conference on Artificial Neural Networks*, pp. 185–198, Springer, 2015.
- [13] M. Lawitzky, M. Kimmel, P. Ritzer, and S. Hirche, "Trajectory generation under the least action principle for physical human-robot cooperation," in *Proceedings of the IEEE International Conference on Robotics and Automation (ICRA)*, 2013.
- [14] E. You and K. Hauser, "Assisted teleoperation strategies for aggressively controlling a robot arm with 2D input," in *Proceedings of Robotics: Science and Systems*, vol. 7, 2012.
- [15] S. Gulati, C. Jhurani, B. Kuipers, and R. Longoria, "A framework for planning comfortable and customizable motion of an assistive mobile robot," in *Proceedings in the IEEE/RSJ International Conference on Intelligent Robots and Systems (IROS)*, 2009.
- [16] Y. Uno, M. Kawato, and R. Suzuki, "Formation and control of optimal trajectory in human multijoint arm movement," *Biological Cybernetics*, vol. 61, no. 2, pp. 89–101, 1989.
- [17] T. Flash and N. Hogan, "The coordination of arm movements: an experimentally confirmed mathematical model," *The Journal of Neuroscience*, vol. 5, no. 7, pp. 1688–1703, 1985.

- [18] E. Todorov, "Optimality principles in sensorimotor control," *Nature neuroscience*, vol. 7, no. 9, pp. 907–915, 2004.
- [19] S. M. Khansari-Zadeh and A. Billard, "Learning stable nonlinear dynamical systems with gaussian mixture models," *IEEE Transactions on Robotics*, vol. 27, no. 5, pp. 943–957, 2011.